Advanced Materials Research *Online: 2014-08-11*
ISSN: 1662-8985, Vol. 996, pp 112-117
doi:10.4028/www.scientific.net/AMR.996.112

New modelling approach for micromechanical modelling of the elastoplastic behaviour

Jamal Fajoui[1,a*], David Gloaguen[1,b], Amel Alimi[1,2,c], Mohamed Kchaou[2,d], Frédéric Jacquemin[1,e], Riadh Elleuch[2,f]

[1] Université de Nantes, Institut de Recherche en Génie Civil et Mécanique (UMR CNRS 6183), 58, rue Michel Ange - BP 420, 44606 Saint-Nazaire Cedex, France

[2] Laboratoire des Systèmes Electro-Mécaniques (LASEM), Ecole Nationale d'Ingénieurs de sfax, 3038 Sfax, Tunisie

[a*]: jamal.fajoui@univ-nantes.fr, [b]: david.gloaguen@univ-nantes.fr, [c]: amel.alimi@yahoo.fr, [d]: kchaou.mohamed@yahoo.fr, [e]: Frederic.jacquemin@univ-nantes.fr, [f]: riadh.elleuch@gnet.tn

Keywords: mechanical behavior, plasticity, dislocation, neutron diffraction, homogenization, self-consistent model, biphasic model

Abstract. A new theoretical approach is developed to simulate the elastoplastic behaviour in cubic alloys during various strain-path changes. The polycristal is considered as a composite consisting of hard dislocation walls of high local dislocation density which are separated by soft regions of low local dislocation density. The improved elasto-plastic self-consistent method is applied to deduce the global behaviour of the aggregate. The model is tested by simulating the macroscopic behavior and the development of intergranular strains during different complex loads.

Introduction

During sheet metal forming, the material undergoes complex mechanical loadings that can dramatically affect the mechanical performances and the lifetime of metallic product. Optimizing such technologies requires a deep knowledge of the mechanical behaviors at different levels.

Recent improvements in mechanical deformation modelling enable more readily predictions of the global and the internal stress propagation [1]. This modelling is positioned on microscopic scale and seeks to make the link with the macroscopic one using and developing the homogenization approach like the self-consistent model. The polycristal is considered as a inclusion set embedded in a homogeneous medium equivalent (HME). The evolution of microstructure is highlighted by a hardening matrix with phenomenological approach.

In this work, new homogenization approach is developed to predicted the elastoplastic behavior taking into account the evolution of a dislocation microstructure. The polycrystalline aggregate is considered as a two-phase material: dislocation walls “w” (with high dislocation density) and dislocation cells “c” (with low dislocation density). The grain boundaries are assimilated to dislocation walls. Considering a two-phase composite material, the material can be equivalently represented as an inclusion (cell or wall) embedded in an HME. A meso-macro transition using a self-consistent model is used to deduce the macroscopic behaviour of the polycrystal. The intragranular heterogeneities are taken into account by a new hardening formulation linked to the two-phase description. The expressions of the hardening laws and the local elastoplastic behaviour have been determined taking into account internal variables like dislocation densities on each deformation system, phase and volume fraction of the cells. The Fig. 1 illustrate the composite model developed in this work.

In order to verify the model, different experimental results with complex loading paths on single crystals and polycrystals have been used here. In this paper, the composite approach is considered for an austenitic stainless steel (AISI 316L).

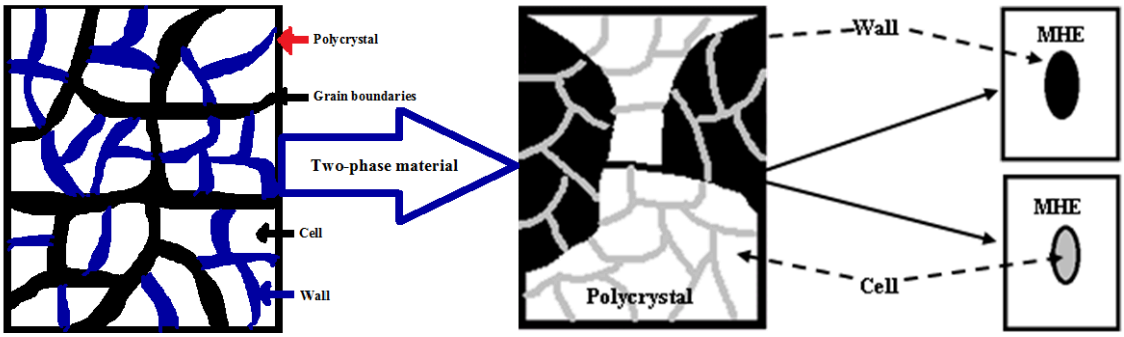

Fig. 1. Schematic diagram showing the composite approach

Experimental

Samples were tested using the ENGIN-X beamline at the ISIS facility, Rutherford Appleton Laboratory (Didcot, UK) [2], using a 50 kN Instron testing machine. Briefly, the ENGIN-X instrument presents a horizontal loading axis positioned at 45° to the incident beam. Two detector banks are set up horizontally and at angles ±90° to the incident beam, allowing simultaneous measurements of lattice strains in both parallel (loading direction denoted LD) and perpendicular (transverse direction, TD) directions to the applied load, in the opposing 90° detector banks. The time-of-flight technique enables collection of an entire diffraction pattern (effective d-spacing range from 0.88 to 2.63Å) in each detector simultaneously, owing to the specificity of the neutron beam. The detector banks cover ± 14° in the horizontal plane and ±21° in the vertical plane [2]. The gauge volume was 4 x 4 x 4 mm^3, and the recording time was taken over 15 min for each measurement at a given macroscopic strain. Macroscopic strain was monitored on the sample using a clip gauge. Single peak fitting was performed using the Open Genie code [3].

Tension-compression tests (Bauschinger reversal tests), were performed at room temperature. We consider two pre-strains: 2 and 6% in tension mode for the first test, and, -2% and -3% in compression mode for the second one. In situ diffraction volume analyses were performed in order to follow the evolution of intergranular strains during complex loading (tension-compression) at different strain rates with an interval of 0.5 %. Experimental results were obtained for several refelection : (111), (200), (220), (311), (331), (420), (422) and (511). For a more detailed description of ND, see Ref. [4].

Model

The elastoplastic self-consistent model (EPSC model) is based on a representation of the material at several scales. On one hand, the ‘‘local” scale denoted by the superscript II, where one observes the behaviour of each constituent, considered as an ellipsoidal and homogeneous inclusion (also called Base Volume or BV). On the other hand, the macroscopic scale denoted by the superscript I, where one can observe the behavior of the HME. As elastoplastic behavior is considered here, it is expressed by the following law:

$$\dot{\sigma}^{I} = L^{I}\dot{\varepsilon}^{I} \quad (1)$$

$$\dot{\sigma}^{I\alpha} = L^{\alpha}\dot{\varepsilon}^{I\alpha} \quad (2)$$

$$\dot{\sigma}^{II\alpha} = \ell^{\alpha}\dot{\varepsilon}^{II\alpha} \quad (3)$$

The subscript ‘α’ stands for walls ‘w’ and cells ‘c’. L^{I} (resp. L^{α}) is the macroscopic tangent moduli tensors corresponding to polycristal (resp. to phase α). ℓ^{α} is the microscopic tangent moduli tensors for each phase.

The slip systems are defined by the unit normal to the slip plane n_{α}^{g} and the slip direction m_{α}^{g}. If $\dot{\gamma}_{\alpha}^{g}$ denotes the slip rate on active system g, the plastic strain rate $\dot{\varepsilon}^{p\alpha}$ is given by:

$$\dot{\varepsilon}^{pII\alpha} = \sum_g R_\alpha^g \dot{\gamma}_\alpha^g \quad (4)$$

where R_α^g is the Schmid tensor on a system g. $\dot{\gamma}_\alpha^g$ denotes the slip rate on a system g.

The elastic strain rate is linked to the stress rate in the grain through the Hooke's law:

$$\dot{\varepsilon}^{eII\alpha} = \dot{\varepsilon}^{II\alpha} - \dot{\varepsilon}^{pII\alpha} = s : \dot{\sigma}^{II\alpha} \quad (5)$$

where s is the elastic compliance tensor at the grain level. A:B denotes the double scalar product $A_{ijkl}B_{klmn}$ using the Einstein summation convention.

The main mechanism responsible of the hardening involves dislocations that generated inside grains and built a particular architecture. These structures could be viewed as composites consisting of hard dislocation walls having high local dislocation density, separated by soft regions (cells) having low local dislocation density. Based on these physical processes, we defined the rate of increase of dislocations density inside the cells and the walls on a slip system g is:

$$\dot{\rho}_\alpha^g = \dot{\rho}_\alpha^{g+} + \dot{\rho}_\alpha^{g-} \text{ with: } \dot{\rho}_\alpha^{g+} = \frac{1}{bL^g}\dot{\gamma}_c^g,\ \dot{\rho}_\alpha^{g-} = -\frac{2y_c}{b}\rho_\alpha^g\dot{\gamma}_\alpha^g \text{ and } L_\alpha^g = \frac{k_L}{\sqrt{\sum_{h\neq g}\rho_\alpha^h}} \quad (6)$$

$\dot{\rho}_\alpha^{g+}$ corresponds to the rate of increase of dislocation density inside the walls on the system g. This term is responsible for the creation and the development of the wall and the cell structure.

$\dot{\rho}_\alpha^{g-}$ is the annihilation term which takes into account the dynamic recovery during the deformation.

b is the magnitude of the Burgers vector and y_c is proportional to the annihilation distance of dislocation dipoles. L^g is the mean free path of mobile dislocations in the cell interiors associated to the deformation system g. Its evolution is governed by the density of point obstacles (essentially cell walls) cutting the system g and creating interactions with gliding dislocations.

The critical resolved shear stress (CRSS) can be related to the dislocations densities by the hardening relation:

$$\tau_{c\alpha}^g = \tau_{c0\alpha}^g + \xi\mu b\sqrt{\sum_h a^{gh}\rho_\alpha^h} \quad (7)$$

$\tau_{c0\alpha}^g$ is the initial reference shear stress on system g and ξ is a constant depending on the interaction of dislocations ($\xi \in [0.25\text{-}0.6]$). a^{gh} is a hardening matrix which terms depend on the type of interactions between dislocation families g and h. Only two terms, a^{gg} and $a_{g\neq h}^{gh}$ (respective self- and latent hardening parameters), will be considered. ρ_α^h is the dislocation density in the phase α.

By developing (8), we obtain:

$$\dot{\tau}_{cc}^g = \frac{\xi^2\mu^2 b}{2(\tau_{cc}^g - \tau_{c0c}^g)}\frac{a^{gh}}{L_c^h}\dot{\gamma}_c^h - \frac{y_c\xi^2\mu^2 b}{(\tau_{cc}^g - \tau_{c0c}^g)}a^{gh}\rho_c^h\dot{\gamma}_c^h \quad (8)$$

$$\dot{\tau}_{cw}^g = \frac{\xi^2\mu^2 b}{2(\tau_{cw}^g - \tau_{c0w}^g)}\frac{a^{gh}}{L_w^h}\dot{\gamma}_c^h - \frac{y_c\xi^2\mu^2 b}{(\tau_{cw}^g - \tau_{c0w}^g)}a^{gh}\rho_w^h\dot{\gamma}_w^h \quad (9)$$

The plastic flow can take place in a grain when the Schmid criterion is verified, i.e. slip occurs if the resolved shear stress τ_α^g on a system g, for each phase, is equal to the critical value $\tau_{c\alpha}^g$ depending on the hardening state of the slip system. This necessary condition is insufficient, and the complementary condition, which states that the increment of the resolved shear stress must be equal to the incremental rate of the critical resolved shear Stresses (CRSS), has to be checked simultaneously. The resolved shear stress is defined as the projection of the phases stress tensor σ^α on the considered deformation system. In small strain formulation, one has:

$$\tau_\alpha^g = R_\alpha^g : \sigma^\alpha = \tau_\alpha^g \text{ and } \dot{\tau}_\alpha^g = R_\alpha^g : \dot{\sigma}^\alpha = \dot{\tau}_\alpha^g \quad (10)$$

We used another formulation to resolve the problem of ambiguous selection of deformation systems and reduce the running time of computations [1, 6]. The slip rate can be expressed by the following equation:

$$\dot{\gamma}_\alpha^g = K_\alpha^g \dot{\tau}_\alpha^g \tag{11}$$

The slip rates ($\dot{\gamma}_c^g$ and $\dot{\gamma}_w^g$) are linked to the resolved shear stress rates ($\dot{\tau}_c^g$ and $\dot{\tau}_w^g$) through a hyperbolic tangent function K_α^g. This function depends on the $\tau_{c\alpha}^g$ and τ_α^g. Hence, it's able to describe the hardening behavior during the plastic regime. By developing (1) - (11), one obtains after calculations the following matrix form:

$$\dot{\gamma}_\alpha^g = \sum_h \left(\delta_{gh} + K_\alpha^g R_\alpha^g : c : R_\alpha^h\right)^{-1} K_\alpha^h R_\alpha^h : c : \dot{\varepsilon}^{II\alpha} \tag{12}$$

After some mathematics development, a linear relation is obtained:

$$\dot{\varepsilon}^{II\alpha} = \left[s + \sum_g K_\alpha^g R_\alpha^g R_\alpha^h\right] : \dot{\sigma}^{II\alpha} = \ell^{\alpha\,-1} : \dot{\sigma}^{II\alpha} \tag{13}$$

From (14), we deduce the expression of microscopic tangent moduli tensors as follow:

$$\left[s + \sum_g K_\alpha^g R_\alpha^g R_\alpha^h\right] = \ell^{\alpha\,-1} \tag{14}$$

The relations between local and global strains and stresses can be expressed through:

$$\dot{\varepsilon}^{II\alpha} = \left[I + S^{esh} : L^{I\,-1} : (\ell^\alpha - L^I)\right]^{-1} : \dot{\varepsilon}^I \tag{15}$$

$$\dot{\sigma}^{II\alpha} = \ell^\alpha : \left[I + S^{esh} : L^{I\,-1} : (\ell^\alpha - L^I)\right]^{-1} : L^{I\,-1} : \dot{\varepsilon}^I \tag{16}$$

Where S^{esh} is the Eshelby tensor. The localization and concentration tensors (inclusion-phase) are calculated from:

$$\dot{\varepsilon}^{II\alpha} = \left[I + S^{esh} : L^{\alpha\,-1} : (\ell^\alpha - L^\alpha)\right]^{-1} : \dot{\varepsilon}^{I\alpha} \tag{17}$$

$$\dot{\sigma}^{II\alpha} = \ell^\alpha : \left[I + S^{esh} : L^{\alpha\,-1} : (\ell^\alpha - L^\alpha)\right]^{-1} : L^{\alpha\,-1} : \dot{\varepsilon}^{I\alpha} \tag{18}$$

The scale transition relations are basically written as volume averages operations on stresses and strains. Hill [8, 10, 11] showed, in a very general way, the equivalence between set (i.e., volume) averages and volume integrals. Hill's volume average relations over the mechanical states (also called consistency principles on mechanical states) are written:

$$\dot{\sigma}^I = \langle \dot{\sigma}^{II\alpha} \rangle \text{ and } \dot{\sigma}^\alpha = \langle \dot{\sigma}^{II\alpha} \rangle_\alpha \tag{19}$$

$$\dot{\varepsilon}^I = \langle \dot{\varepsilon}^{II\alpha} \rangle \text{ and } \dot{\varepsilon}^\alpha = \langle \dot{\varepsilon}^{II\alpha} \rangle_\alpha \tag{20}$$

where the square brackets <…> represent the volume average.

By combining between (15)-(20), one obtain:

$$\dot{\sigma}^I = \langle \ell^\alpha : \left[I + S^{esh} : L^{I\,-1} : (\ell^\alpha - L^I)\right]^{-1} : L^{I\,-1} \rangle : \dot{\varepsilon}^I = L^I : \dot{\varepsilon}^I \tag{21}$$

$$\dot{\sigma}^\alpha = \langle \ell^\alpha : \left[I + S^{esh} : L^{\alpha\,-1} : (\ell^\alpha - L^\alpha)\right]^{-1} : L^{\alpha\,-1} \rangle_\alpha : \dot{\varepsilon}^{I\alpha} = L^\alpha : \dot{\varepsilon}^{I\alpha} \tag{22}$$

Therefore:

$$L^I = \langle \ell^\alpha : \left[I + S^{esh} : L^{I\,-1} : (\ell^\alpha - L^I)\right]^{-1} : L^{I\,-1} \rangle \tag{23}$$

$$L^\alpha = \langle \ell^\alpha : \left[I + S^{esh} : L^{\alpha\,-1} : (\ell^\alpha - L^\alpha)\right]^{-1} : L^{\alpha\,-1} \rangle_\alpha \tag{24}$$

Eq. (23) (resp. (24)) is a non-linear implicit equation because S^{esh} depends on the unknown L^I (resp. L^α). This equation is solved by iteration. Once L^I is known, by specifying an overall stress or

strain, the model can give the corresponding stress or strain tensors for each orientation. Therefore, we can describe the mechanical response of the polycrystal.

After some mathematics development, we find the relation between L^I and L^α as follow:

$$L^\alpha = \langle \ell^\alpha : [I + S^{esh} : L : (\ell^\alpha - L^I)]^{-1} \rangle_\alpha : \langle [I + S^{esh} : L^I : (\ell^\alpha - L^I)]^{-1} \rangle_\alpha^{-1} \quad (25)$$

Results

The Bauschinger effect, present in an austenitic stainless steel (AISI 316L), is simulated using this approach. These simulations are used to test the model's ability to simulate complex loading (traction-compression) at different levels. Simulation results will be compared with those from the experimental tests of neutron diffraction.

The simulations refer to the polycrystalline aggregate consisting from 1000 crystallites. The texture is determined from the neutron diffraction tests in GEM beamline at the ISIS facility. The elastic properties are considered as isotropic (μ = 70 GPa and ν = 0.3). The grains were assumed to be equiaxed. The material parameters have been determined by fitting the experimental monotonic tensile curve (Fig.1.a). The parameters values are listed in Table 1.

Table 1. Simulation parameters

τ_{c0c}^g (MPa)	τ_{c0w}^g (MPa)	ξ	k	y_c (m)	ρ_c^h (m)	ρ_w^h (m)	a^{gh}	a^{hh}	f
195	245	0,35	20	$2{,}8510^{-9}$	10^9	10^{12}	1,2	1	0,65

Fig.1.a. shows the evolution of the macroscopic tangent moduli tensors during the first loading using the present approach and the classical Elastoplastic Self-Consistent model (EPSC) [1, 6]. They give the same result for this tensor. It will enable us to conclude that the present model can deliver positive results like the EPSC one in monotonic loading.

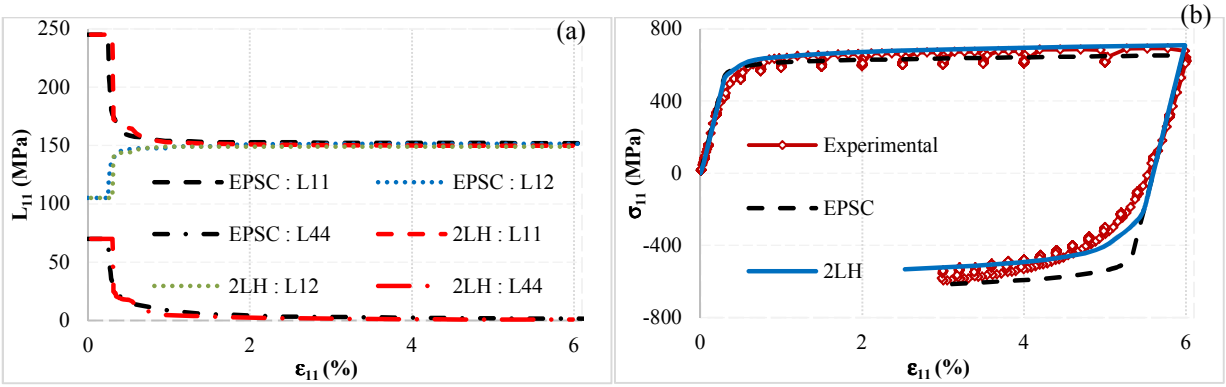

Fig.1: a. Comparison between experimental and simulated stress-strain curves during complex load path; b. The evolution of the macroscopic tangent moduli tensors

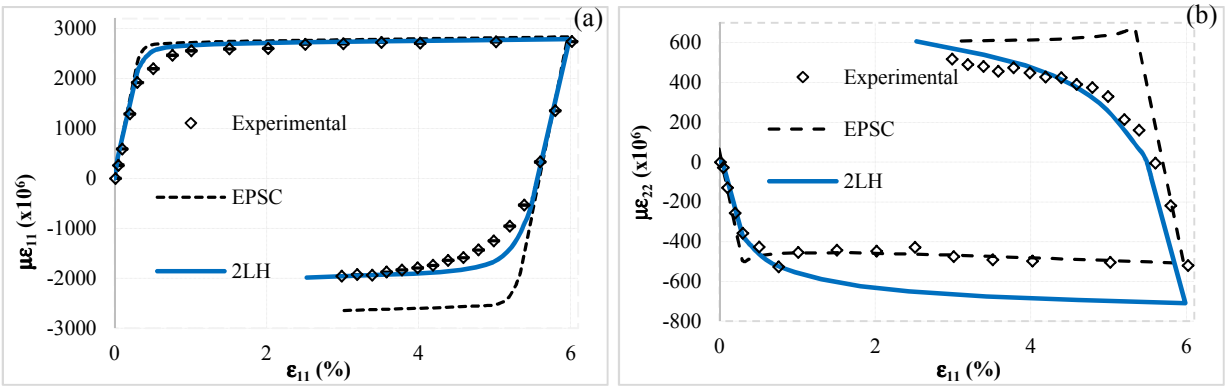

Fig.2. Experimental and simulated results for diffracting volume ({111} reflection) behavior during sequential loading tests

Fig.1.b. illustrates the simulation results for tension-compression tests using two differents schemes: the EPSC and the present approach. The EPSC scheme fails to explain and reproduce correctly the softening effects during the compression loading. This method weakly takes into account the formation, the evolution and the stability of induced dislocations microstructures which are strongly path dependent. One can observed in Fig. 1.b. that the present model captures all the essential features (reloading yield stress, macroscopic work hardening) associated with the Bauschinger effect. These comparisons show that the difference can be explained by the internal stresses due to the first uniaxial loading.

Fig.2. gives the volume diffracting behavior of (111) crystallographic plane for the present model and the EPSC one. We have simulated the transversal and the longitudinal behaviors during the Bauschinger loading. For the present model, a correct agreement is observed between the simulations and the experimental results at the diffracting volume.

Conclusion

In this paper, we developed a new model to simulate the elastoplastic mechanical behavior of metallic materials with cubic structure. The polycristallin aggregate is considered as a two-phase composite: i) hard phase (wall) with high density dislocation; ii) soft phase (cell) with low density dislocation. Therefore, a new hardening law is proposed taking account the evolution of the microstructure of dislocation and other internal parameters responsible of plasticity.

This approach has been developed in order to simulate the mechanical response of cubic alloys with two-stage strain path experiments. Correct agreement is observed between the simulation data and the experimental results at the meso- and the macroscopic levels. Strains observed by neutron diffraction is significantly different from one plane family to another. These results can be explained by the presence of plastic anisotropy. Our new approach has captured the differences between these lattice plane families.

References

[1] D. Gloaguen, G. Oum, V. Legrand, J. Fajoui, S. Branchu, Experimental and theoretical studies of intergranular strain in an alpha titanium alloy during plastic deformation, Acta Materialia, 61, 15, (2013), 5779-5790.
[2] J. R. Santisteban, M.R. Daymond, J.A. James, L. Edwards, ENGIN-X: a third-generation neutron strain scanner, J. A. Crystallographic, 39, (2006), 812-825.
[3] C. M. Moreton-Smith, S. D. Johnston, F.A. Akeroyd, Open-GENIE, a generic, multi-platform program for the analysis of neutron scattering data, J Neutron Res, 4, (1996), 41-47.
[4] W. Kockelmann, L. C. Chapon, P. G. Radelli, Neutron texture analysis on GEM at ISIS, Physica B, 385, (2006), 639-643.
[5] H. Mughrabi, The long-range internal stress field in the dislocation wall structure of persistent slip bands, Phys Stat Sol (a) 104, (1987), 107-120.
[6] J. Fajoui, D. Gloaguen, B. Courant, R. Guillen, Micromechanical modelling of the elastoplastic behaviour of metallic material under strain-path changes, C. Mechanics, 44, (2009), 285-296.
[7] E. Kröner, On the plastic deformation of polycrystals. A. Metallurgica, 9, (1961), 155-161.
[8] R. Hill, The essential structure of constitutive laws for metals composites and polycrystals, J. M. P. Solids, 15, (1967), 79-95.
[9] J. D. Eshelby, The Determination of the Elastic Field of an Ellipsoidal Inclusion, and Related Problems, Proceedings of the Royal Society London A241, (1957), 376-396.
[10] J. W. Hutchinson, Elastic-plastic behaviour of polycrystalline metals and composites, Proc. R. Soc., 319 A, (1970), 247-272.
[11] R. Hill, Continuum micromechanics of elastoplastic polycrystals, J. Mech. Phys. Solids, 13, (1965), 89-101.